CONF-950801--18

BNL- 61739

X-RAY SPECTROSCOPIC STUDIES OF MICROBIAL TRANSFORMATIONS OF URANIUM*

Cleveland J. Dodge and Arokiasamy J. Francis
Department of Applied Science
Biosystems and Process Sciences Division
Brookhaven National Laboratory
Upton, NY 11973

and

Clive R. Clayton
Department of Materials Science and Engineering
SUNY-SB
Stony Brook, NY 11794-2275

October 1995

To be published in
"Application of Synchrotron Radiation in Industrial, Chemical, and Material Science"
L. J. Terminello, K. L. D'Amico, and D. K. Shuh, Editors
Plenum Publishing, NY

*Presented at the 210th American Chemical Society Meeting, August 20-24, 1995.

X-RAY SPECTROSCOPIC STUDIES OF MICROBIAL TRANSFORMATIONS OF URANIUM

Cleveland J. Dodge[1], Arokiasamy J. Francis[1], and Clive R. Clayton[2]

[1]Brookhaven National Laboratory
Department of Applied Science
Upton, NY 11973
[2]SUNY at Stony Brook
Department of Materials Science and Engineering
Stony Brook, NY 11794

INTRODUCTION

The presence of radionuclide and toxic metal contaminants at Department of Energy (DOE) sites is a major environmental concern. Uranium, in particular is of interest due to its presence in soils, sediments, and wastes resulting from nuclear weapons production. Characterization of uranium in these materials is necessary so that appropriate treatment strategies can be developed. Information on X-ray spectroscopic analysis of uranium has been limited to oxides[1], intermetallic compounds[2], and encapsulated forms[3,4]. In this study a systematic approach was undertaken to characterize various uranium compounds in order to elucidate the basic mechanisms involved in remediation of contaminated sites. We used X-ray photoelectron spectroscopy (XPS) and X-ray absorption near edge structure (XANES) to determine valence state, and extended X-ray absorption fine structure (EXAFS) to determine compound structure.

MATERIALS AND METHODS

Compounds

The following uranium compounds U-metal (α-phase), UO_2, U_3O_8, γ-UO_3, uranyl acetate, uranyl nitrate, uranyl sulfate (Atomergic Chemicals, Farmingdale NY), aqueous and solid forms of 1:1 U:citric acid and 1:1:2 U:Fe:citric acid mixed-metal complexes, and a precipitate obtained by photodegradation of the U-citrate complex were used.

Equimolar 1:1 U(VI):citric acid complex was prepared by combining equal volumes of uranyl nitrate and citric acid (pH 6.0) solutions, in a beaker with continous stirring. The pH

was adjusted to 6.0 with sodium hydroxide and the ionic strength was maintained at 0.1 M by adding KCl. The 1:1:2 U(VI):Fe(III):citric acid complex was prepared in a similar fashion using uranyl nitrate, ferric nitrate, and citric acid. The final concentration of each complex was 6.5 mM. Iron and U stock solutions were standardized by visible spectrophotometry, and citric acid by high pressure liquid chromatography. Solid forms of the U- and U-Fe-citrate complexes were prepared by crystallization from the aqueous state. Uranium precipitate from photodegradation of U-citrate complex was collected after exposure of the aqueous complex to a light intensity of 0.04 mEinstein m^{-2} s^{-1} in an incubator at 26±1°C[5].

Uranium contaminated sludge and sediment samples were obtained from Y-12 Plant, Oak Ridge, TN. To determine the extent of uranium transformations in the waste due to anaerobic microbial activity, samples were inoculated with *Clostridium* sp. (ATCC 53464) and incubated for several days[6]. Speciation of uranium in the waste material before and after microbial treatment was determined by XPS and XANES.

Uranium Characterization

XPS. A VG Scientific ESCA MK II spectrometer at SUNY-Stony Brook was used to determine peak positions at the U $4f_{7/2}$ and U $4f_{5/2}$ binding energy of U-metal, UO_2, U_3O_8, γ-UO_3, uranyl acetate, uranyl nitrate, and uranyl sulfate[7]. The shift in peak position with oxidation state due to changes in uranium binding energy was determined after curve fitting.

XANES. XANES, usually within 40 eV of the absorption edge, provides data on the local structure and oxidation state of uranium. U-metal, UO_2, γ-UO_3, and uranyl acetate were analyzed at the National Synchrotron Light Source (NSLS) on beam line X-19A. The sample was mounted on Mylar foil and the XANES spectrum was collected at the M_V absorption edge (3.545 keV) using an electron yield detector and a double-crystal Si(111) monochromator[7]. The spectrum was normalized after background subtraction, the curve was fitted using a least-squares program, and the absorption peak maximum of the sample determined. XANES information at the L_{III} edge was collected for hexavalent uranium γ-UO_3, uranyl acetate, and 1:1 U:citric acid and 1:1:2 U:Fe:citric acid complexes.

EXAFS. EXAFS measurements provide information on the local three-dimensional environment surrounding a central atom and are obtained using a multi-step analysis procedure to identify nearest neighbor atoms, determine atomic distances, coordination number of central atom, and coordination geometry. This information can be obtained regardless of the physical state of the sample (e.g. solid, aqueous). Solid γ-UO_3, uranyl nitrate, uranyl acetate, ferric acetylacetonate, and equimolar U:citric acid and U:Fe:citric acid complexes were mixed with boron nitride (10% w/v), placed in heat sealed polypropylene bags (0.2 mil) and analyzed on beamline X-23A2 at the NSLS using a fluorescence detector at the uranium L_{III} edge (17.165 keV) and at the iron K edge (7.1112 keV). Aqueous U-citrate complexes were transferred to polypropylene bags and analyzed. Data was analyzed using the UW EXAFS analysis software MacXAFS 3.6.

RESULTS AND DISCUSSION

XPS. Table 1 shows the U $4f_{7/2}$ and U $4f_{5/2}$ binding energies for U-metal, UO_2, U_3O_8, γ-UO_3, uranyl acetate, uranyl nitrate, and uranyl sulfate. Uranium metal exhibited the lowest binding energy at 376.6 eV for the U $4f_{7/2}$ spin state. With increase in oxidation state to +4 for uranium dioxide, the binding energy increased to 380.4 eV. The +6 oxidation state however, exhibited a range of energies from 381.9 eV for uranium trioxide to 382.2 eV for uranyl

Table 1. Peak binding energies for uranium 4f electrons in model compounds.

Compound	Oxidation state	Binding energy (eV) U $4f_{7/2}$	U $4f_{5/2}$
U metal	0	376.6	387.1
UO_2	+4	380.4	391.3
U_3O_8	+4	381.5	392.5
	+6	382.9	394.1
γ-UO_3	+6	381.9	391.9
Uranyl acetate	+6	381.5	392.4
Uranyl nitrate	+6	382.0	392.1
Uranyl sulfate	+6	382.2	395.5

sulfate. In the mixed-valent uranium oxide, U_3O_8, two peaks at 381.5 and 382.9 eV were fitted to the main peak envelope; these were due to the presence of +4 and +6 oxidation states, respectively. There was a larger shift in the U $4f_{7/2}$ peak for +6 uranium compared to the pure hexavalent compounds. There also was a large shift in binding energy for the U $4f_{5/2}$ spin state of uranyl sulfate. These differences may be a result of the coordination geometry of the oxygens which increase the effective charge on the uranium.

The ability of this technique to differentiate oxidation states of uranium is of particular importance in the bioremediation of wastes. We previously showed using XPS that uranium was reduced from the soluble U^{6+} to insoluble U^{4+} and U^{3+} as a result of anaerobic bacterial activity[8]. Microbial reduction of uranium from soluble U^{6+} to insoluble U^{4+} increases its stability in the environment by forming insoluble uranium (IV) species.

XANES. Figure 1 shows the absorption spectra for a series of uranium compounds collected at the M_V and L_{III} edges. Uranium metal at the M_V absorption edge showed a maximum at 3549.6 eV. An increase in oxidation state to U^{4+}, uranium dioxide, resulted in a shift to higher energy of 0.8 eV (3550.4 eV). Analysis of U^{6+} species, uranium trioxide and uranyl acetate, showed an identical shift in absorption to 3551.1 eV. The presence of a shoulder on the high energy side of the hexavalent uranium compounds was attributed to multiscattering processes involving the uranyl ion[1] and it was more pronounced in uranium trioxide than uranyl acetate. In the 1:1 mixture of +4 and +6 uranium the shift was intermediate between the two indicating the XANES spectrum in this region is sensitive to the oxidation state.

The normalized absorption peak maxima for uranyl acetate, uranium trioxide, 1:1 U:citric acid and 1:1:2 U:Fe:citric acid complexes obtained at the uranium L_{III} edge are broad with a low white line ratio compared to the uranium M_V absorption maxima making it difficult to interpret shifts in peak position resulting from changes in oxidation state. This is due to the increased density of states at the 5f (M_V) compared to the 6d (L_{III}) final states[2]. However, the L_{III} uranium edge is useful for obtaining EXAFS information since it is relatively free from interfering absorption edges. The M_V edge exhibits interference due to presence of the

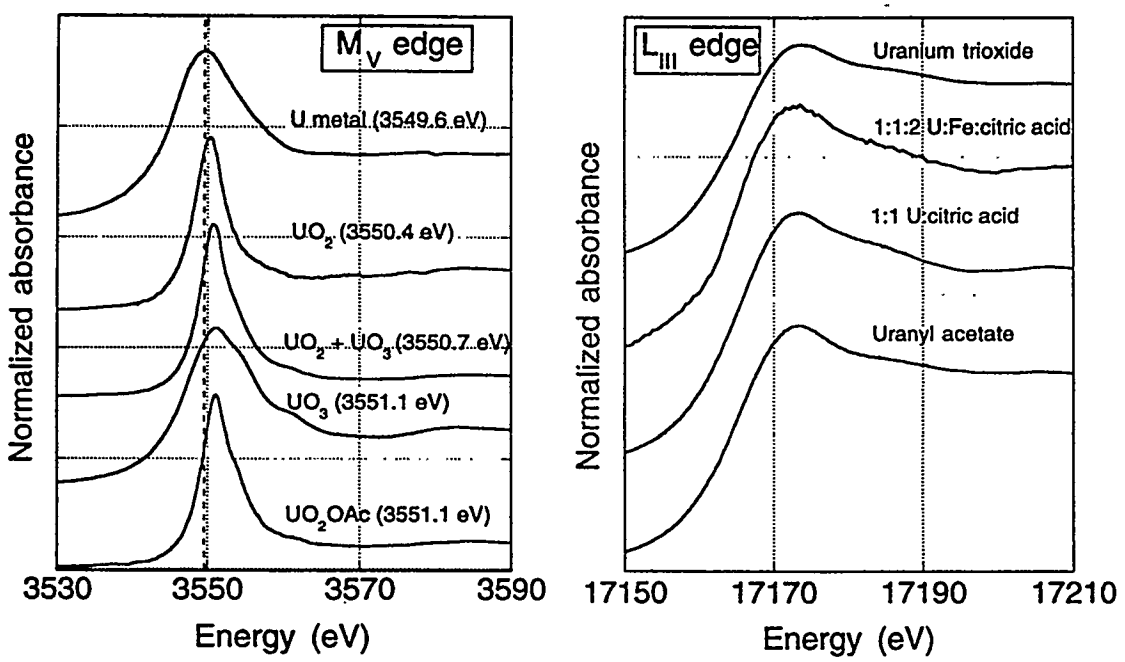

Figure 1. XANES absorption spectra at the M_V absorption edge for compounds of uranium showing a shift in absorption peak maximum with increasing oxidation state, and L_{III} absorption edge for hexavalent uranium compounds. The white line ratio is more pronounced for the M_V compared to the L_{III} absorption edge.

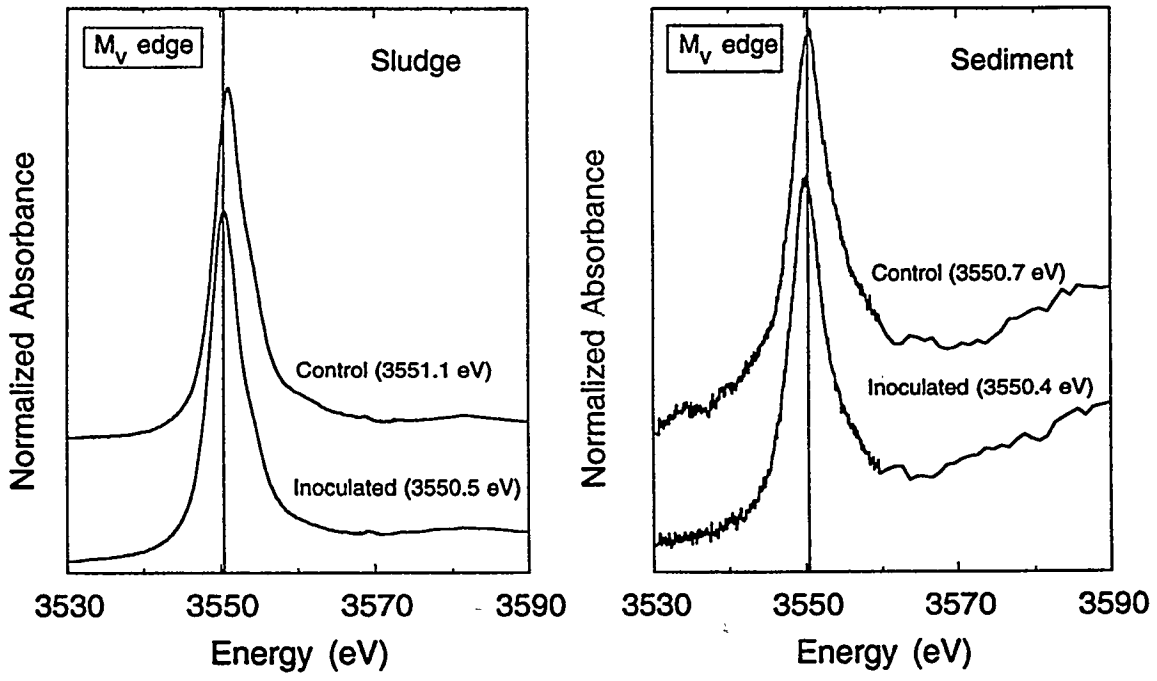

Figure 2. Comparison of XANES absorption spectra at the M_V edge for uninoculated (control) and inoculated samples of sludge and sediment. A decrease in the position of the absorption peak maximum in the bacterially treated samples indicates partial reduction of uranium in the sludge and complete reduction of uranium in the sediment to U^{4+}.

potassium K absorption edge at 3.6078 keV and adjacent U M_{IV} absorption edge at 3.720 keV. Figure 2 shows XANES analyses of the sludge and sediment at the M_V edge before and after bacterial activity. The sludge contained 3080 ppm uranium and the absorption maximum for the untreated (control) sample was 3551.1 eV, indicating that the uranium was predominantly in the hexavalent form. After bacterial treatment there was a shift in the absorption maximum to 3550.5 eV, which is slightly higher than tetravalent uranium (3550.4 eV), but much less than U(VI); this indicates that there was a significant reduction to the U^{4+} state. The sediment contained 640 ppm uranium and the untreated (control) sample exhibited an absorption maximum at 3550.7 eV, which corresponds to a mixture of U^{4+} and U^{6+}. The high organic content (11.3%) may have contributed to maintaining the sediment in a reduced state. In the presence of bacteria the sample peak was shifted to 3550.4 eV, which was identical to U^{4+}, indicating all of the uranium was reduced to the tetravalent state. The reduction of uranium in sludge and sediment by an anaerobic bacterium formed the basis for a unique treatment by enzymatic reduction and subsequent immobilization of the uranium, as well as overall waste volume reduction due to dissolution of the acid soluble components in the waste by the production of organic acid metabolites[9].

EXAFS. ***1:1 U:citric acid complex.*** EXAFS spectra at the uranium L_{III} edge were collected for uranyl acetate and for the solid and aqueous forms of U-citrate complex. Citric acid, a naturally occurring chelating agent which is also present in low-level and transuranic wastes, forms multidentate complexes with metals, and is used to extract uranium and toxic metals from wastes[10]. Uranium forms a stable complex with citric acid which is resistant to biodegradation. It was suggested that the binding of uranium to the hydroxy group of citric acid plays a key role in its stability[11].

Figure 3 compares the Fourier transforms for both the solid and aqueous form of 1:1 U:citric acid complex at pH 6.0 over the k range of 3-14 $Å^{-1}$. The first peak (phase shifted) at 1.8 Å corresponds to the nearest neighbor oxygen ligands of the uranyl ion. Beyond the first shell, information on the aqueous complex is difficult to obtain due to thermal broadening. However, the more ordered solid state shows additional fine structure. The peak at 2.25 Å corresponds to the second shell equatorial oxygen atoms surrounding the uranium. A large amplitude peak also is observed at 5.2 Å. Fourier filtering of the isolated shell displays a large amplitude function with high sinusoidal frequency indicative of the high Z element U (Figure 4). Comparing the backtransformed peak of U-citrate with uranyl acetate dihydrate, a binuclear compound with a $(UO_2)_2(\mu,\eta^2\text{-acetato})_2$ core and a U-U distance of approximately 5.5 Å, shows a similar spectrum (slightly phase shifted), thereby confirming the peak is due to U-U interaction .

Figure 5 shows the k^2 weighted raw EXAFS data after normalization and background subtraction indicating that the U:citric acid complex has a similar structure in both the aqueous and solid state. Although a binuclear structure has been proposed for the complex[12] involving a $(UO_2)_2(\mu\text{-OH})_2$ core, this configuration was based on titration methods and suggests a U-U distance of about 4.1 Å in the complex. EXAFS analysis results shows that the U-U distance in the complex is approximately 5.2 Å. From this data, we propose a new structure consisting of a $(UO_2)_2(\mu,\eta^2\text{-citrato})_2$ core (Figure 6A). The structure is stabilized by the formation of 6 and 7 member rings involving citric acid with uranium.

1:1:2 U:Fe:citric acid complex. The influence of ferric iron, a ubiquitous component in soils and wastes, on the U-citrate complex was investigated to see whether a mixed-metal citrate complex was formed. The ability of citric acid to form complexes with more than one metal has been established[13]. A mixed metal U-Fe complex was confirmed by calorimetric and spectrophotometric methods but its exact structure was not elucidated[14]. Figure 7 shows the Fourier transform spectra of 1:1:2 U:Fe:citric acid at the U L_{III} absorption edge. Absence of a large magnitude peak at 5.2 Å compared to the 1:1 U:citric acid complex indicates ferric iron affects the structure of the U-citrate complex. Fourier-filtering over the k range 3-15 $Å^{-1}$at the

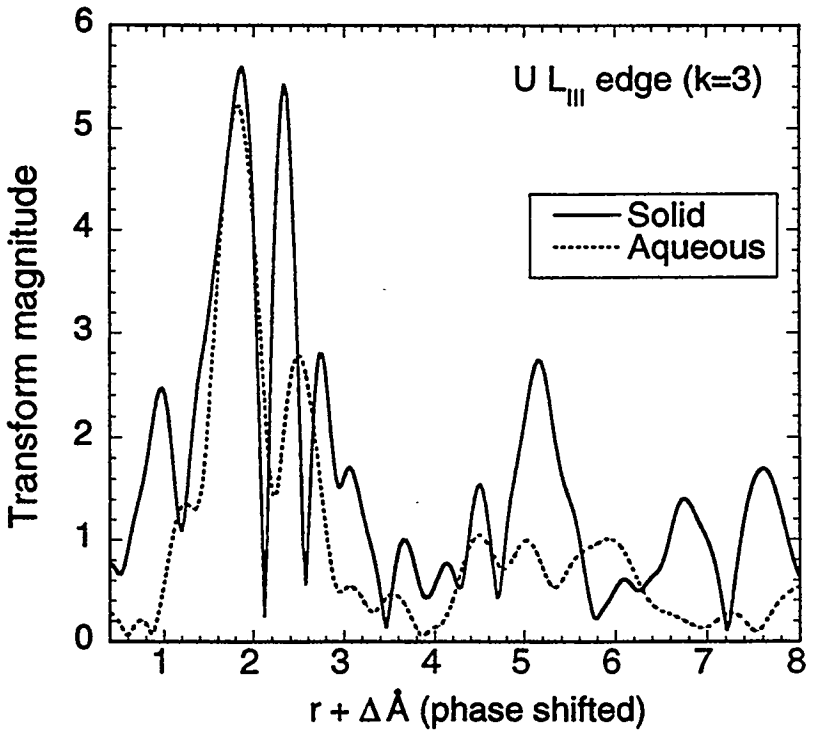

Figure 3. Comparison of phase-shifted Fourier transforms of background-subtracted and k^3-weighted EXAFS spectra of aqueous and solid forms of 1:1 U:citric acid complex at pH 6.0. The large magnitude peak at 5.2 Å for the solid state reveals U-U interaction.

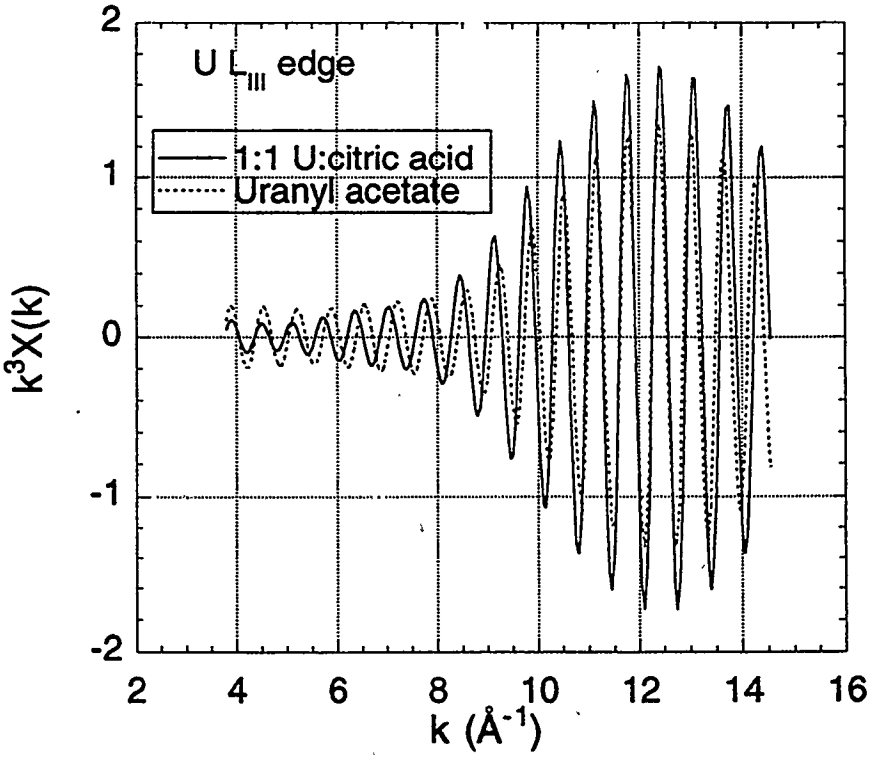

Figure 4. Comparison of Fourier-filtered EXAFS spectra of isolated shells of 1:1 U:citric acid 5.2 Å and uranyl acetate at 5.5 Å plotted as $k^3\chi(k)$ vs. k($Å^{-1}$). The high frequency function, as well as the large amplitude peak at high k, indicate the presence of uranium.

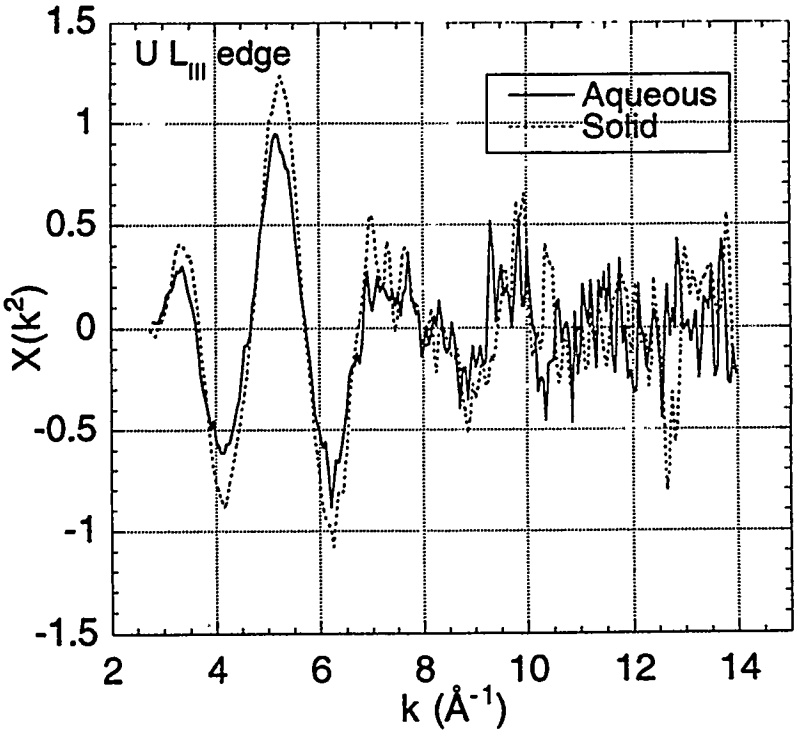

Figure 5. Normalized and background-subtracted EXAFS spectra shown as $\chi(k^2)$ vs. k ($Å^{-1}$) at the L_{III} edge for aqueous and solid forms of 1:1 U:citric acid complex. The similarity in the beat pattern indicates that there is no difference in structure between the two states.

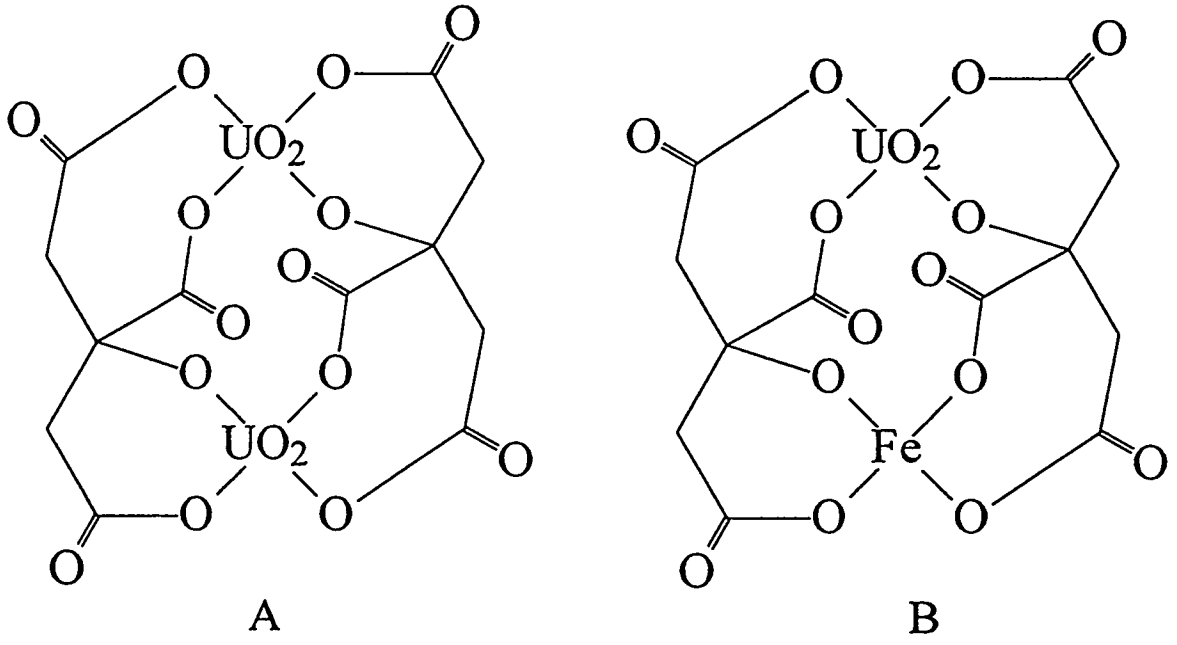

Figure 6. Proposed structures for 1:1 U:citric acid (A) and 1:1:2 U:Fe:citric acid mixed metal (B) complexes based on EXAFS analysis of U-U and Fe-U interactions at 5.2 and 4.8 Å, respectively.

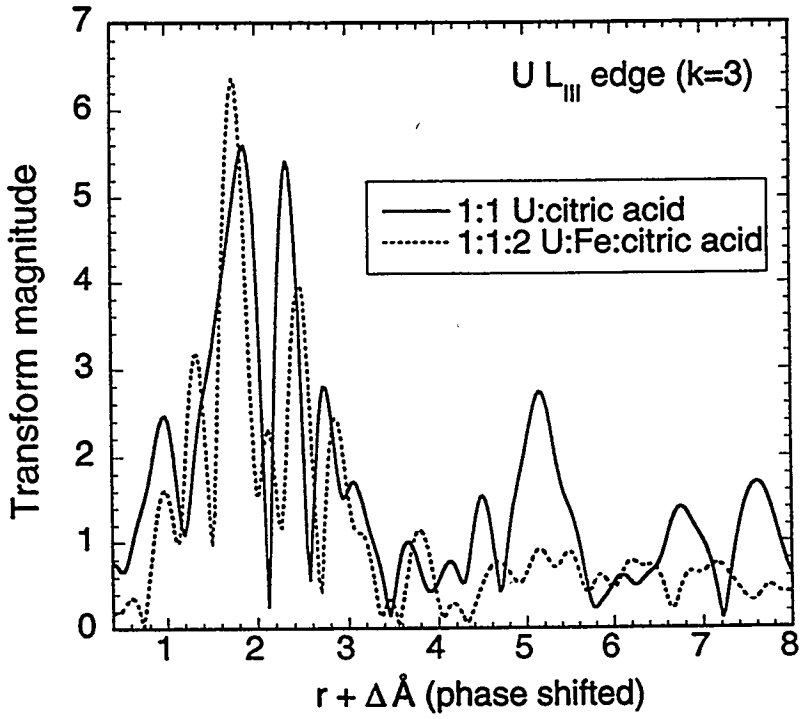

Figure 7. Comparison of phase-shifted Fourier transforms of background-subtracted and k^3-weighted EXAFS spectra of solid 1:1 U:citric acid and 1:1:2 U:Fe:citric acid complexes at pH 6.0. The disappearance of large magnitude peak at 5.2 Å in the presence of ferric iron indicates the formation of a mixed-metal complex with U-Fe interaction.

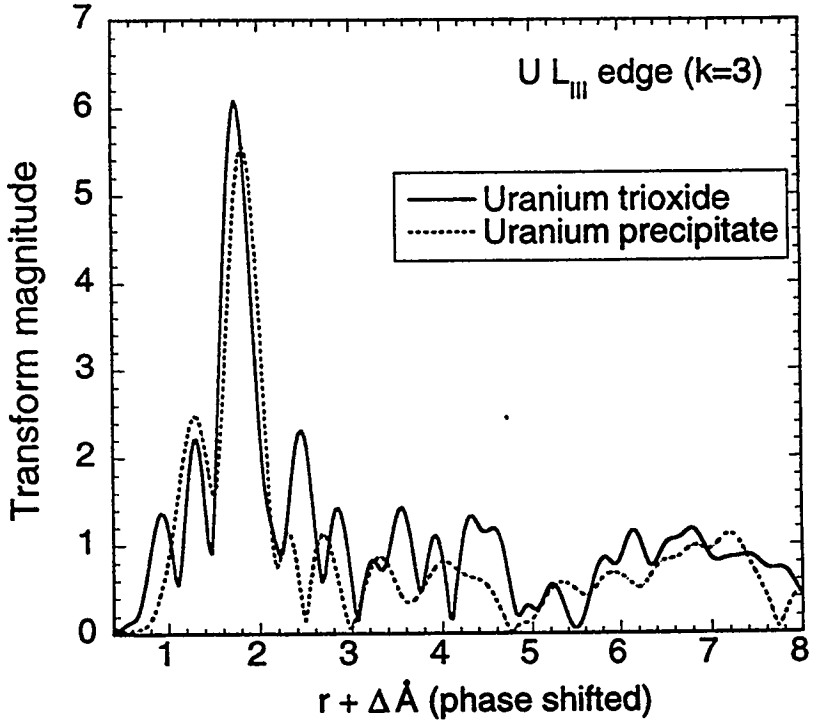

Figure 8. Comparison of phase-shifted Fourier transforms of background-subtracted and k^3-weighted EXAFS spectra of solid uranium precipitate from photodegradation of 1:1 U:citric acid, and uranium trioxide. The lack of structure in the second and third shells for the precipitate suggests that it is slightly amorphous.

Fe edge of the isolated shell at 4.8 Å shows a high frequency function similar to that observed for the U-U interaction (data not shown). These results confirm the presence of a mixed metal binuclear complex with U-Fe distance at 4.8 Å. The difference of 0.4 Å between U-U and U-Fe is approximately the difference in distance for U-O (2.5 Å) and Fe-O (2.0 Å) bonding and indicates that U is replaced by Fe in the complex. Figure 6B shows the proposed structure.

Photochemical Oxidation of Uranyl Citrate Complex. Figure 8 shows the EXAFS spectra of the precipitate obtained from the photochemical degradation of 1:1 U:citric acid complex and uranium trioxide at the L_{III} edge. The structure of the precipitate is similar to uranium trioxide but more amorphous, as revealed by the position of the second and third shells representing the equatorial oxygens surrounding uranium. X-ray diffraction, XPS, and XANES analyses of the precipitate confirmed that it was predominantly uranium trioxide dihydrate with a small amount of the mineral schoepite[5]. The formation of this insoluble compound suggests that photodegradation is an effective treatment for removing uranium from ssolution complexed with citric acid. The uranium oxide is then collected and disposed of, or recycled.

SUMMARY

Several uranium compounds U-metal (α-phase), UO_2, U_3O_8, γ-UO_3, uranyl acetate, uranyl nitrate, uranyl sulfate, aqueous and solid forms of 1:1 U:citric acid and 1:1:2 U:Fe:citric acid mixed-metal complexes, and a precipitate obtained by photodegradation of the U-citrate complex were characterized by X-ray spectroscopy using XPS, XANES, and EXAFS. XPS and XANES were used to determine U oxidation states. Spectral shifts were obtained at the U $4f_{7/2}$ and U $4f_{5/2}$ binding energies using XPS, and at the uranium M_V absorption edge using XANES. The magnitude of the energy shift with oxidation state, and the ability to detect mixed-valent forms make these ideal techniques for determining uranium speciation in wastes subjected to bacterial action.

The structure of 1:1 U:citric acid complex in both the aqueous and solid state was determined by EXAFS analysis of hexavalent uranium at the L_{III} absorption edge and suggests the presence of a binuclear complex with a $(UO_2)_2(\mu,\eta^2\text{-citrato})_2$ core with a U-U distance of 5.2 Å.

The influence of Fe on the structure of U-citrate complex was determined by EXAFS and the presence of a binuclear mixed-metal citrate complex with a U-Fe distance of 4.8 Å was confirmed.

The precipitate resulting from photodegradation of U-citrate complex was identified as an amorphous form of uranium trioxide by XPS and EXAFS.

ACKNOWLEDGEMENTS

We thank Dr. Lars Furenlid (NSLS) for helpful discussions, Sanjay Kagwade (SUNY-SB) for XPS analysis, and Dr. F.J. Wobber, Program Manager, for continued support. This research was performed under the auspices of the Environmental Sciences Division's Subsurface Science Program, Office of Health and Environmental Research, U.S. Department of Energy, under Contract No. DE-AC02-76CH00016.

REFERENCES

1. G. Kalkowski, G. Kaindl, W.D. Brewer, and W. Krone, Near edge X-ray absorption fine structure in uranium compounds, Phys. Rev. B 35:2667 (1987).

2. J.M. Lawrence, M.L. den Boer, and R.D. Parks, X-ray absorption spectra in rare-earth and uranium intermetallics: localized versus itinerant final states, Phys. Rev. B 29:568 (1984).
3. J. Petiau, G. Calas, D. Petit-Marie, A. Bianconi, M. Benfatto, and A. Marcelli, Localization of 5f states in various uranium and thorium oxides and glasses, J. Phys. 47:C8-949 (1986).
4. W.H. Hocking, A.M. Duclos, and L.H. Johnson, Study of fission product segregation in used CANDU fuel by X-ray photoelectron spectroscopy (XPS) II, J. Nucl. Materials 209:1 (1994).
5. C.J. Dodge and A.J. Francis, Photodegradation of uranium-citrate complex with uranium recovery, Environ. Sci. Technol. 28:1300 (1994).
6. A.J. Francis, C.J. Dodge, J.B. Gillow, and J.E. Cline, Microbial transformations of uranium in wastes, Radiochim. Acta 52/53:311 (1991).
7. C.J. Dodge, A.J. Francis, F. Lu, G.P. Halada, S.V. Kagwade, and C.R. Clayton, Speciation of uranium after microbial action by XANES and XPS, in: "Applications of Synchrotron Radiation Techniques to Materials Science," D. Perry, ed., Materials Research Society, Pittsburgh (1993).
8. A.J. Francis, C.J. Dodge, F. Lu, G. Halada, and C.R. Clayton, XPS and XANES studies of uranium reduction by Clostridium sp., Environ. Sci. Technol. 28:636 (1994).
9. A.J. Francis, C.J. Dodge, and J.B. Gillow, Microbial stabilization and mass reduction of wastes containing radionuclides and toxic metals, US Patent No. 5,047,152, September, 1991.
10. A.J. Francis and C.J. Dodge, Waste site reclamation with recovery of radionuclides and metals, US Patent No. 5,292,456, March, 1994.
11. A.J. Francis, C.J. Dodge, and J.B. Gillow, Biodegradation of metal citrate complexes and implications for toxic-metal mobility Nature 356:140 (1992).
12. K.S. Rajan and A.E. Martell, Equilibrium studies of uranyl complexes. II. Interaction of uranyl ion with citric acid, Inorg. Chem. 4:462 (1965).
13. A. Adin, P. Klotz, and L. Newman, Mixed-metal complexes between Indium(III) and Uranium(VI) with malic, citric, and tartaric acids, Inorg. Chem. 9:2499 (1970).
14. E. Manzurola, A. Apelblat, G. Markovits, and O. Levy, Mixed-metal hydroxycarboxylic acid complexes: Formation constants of complexes of U^{VI} with Fe^{III}, Al^{III}, In^{III}, and Cu^{II}, J. Chem. Soc., Faraday Trans. 1 85:373 (1989).